Resonance in a Superstrate-Loaded Cylindrical-Rectangular Microstrip Structure

Kin-Lu Wong, *Member, IEEE,* Yuan-Tung Cheng, and Jeen-Sheen Row

***Abstract*—The complex resonant frequencies of the cylindrical-rectangular microstrip structure loaded with a dielectric superstrate layer is studied by using a rigorous full-wave analysis and the numerical results are obtained by using the Galerkin's moment method calculation. The numerical convergence for the selected sinusoidal basis functions with and without the edge singularity condition is also discussed. Numerical results for the dependence of the real and imaginary parts of the complex resonant frequencies on the superstrate permittivity and thickness are calculated and analyzed, which are also compared with those obtained for the planar microstrip structure.**

I. Introduction

ONE OF THE major advantages of a microstrip patch antenna is its conformity. Several investigations on this kind of conformal antennas have also been reported recently [1]–[5]. For many applications of the conformal patch antenna to be employed in airborne and spacecraft systems, a dielectric superstrate layer is usually added on the top of the patch to provide protection against environmental hazards, such as rain, hail, and snow. Unfortunately, this superstrate layer also causes great effects on the characteristics of the microstrip structure, which have been indicated in many related reports [6]–[9]. However, these studies are mainly on the case of planar microstrip structures and the investigations on the superstrate-loaded conformal microstrip structure are very scant. Available information for such conformal microstrip structures is therefore very limited. This motivates the present work described in this paper to perform a rigorous full-wave approach to study the complex resonant frequency problem of the superstrate-loaded cylindrical-rectangular microstrip structure, which has not been reported in the open literature. The complex resonant frequencies, which can provide the information of the resonant frequency and quality factor of the microstrip structure, are calculated by using the Galerkin's moment method [10] with the selected sinusoidal basis functions for the unknown surface current density on the curved patch. The numerical convergence for the sinusoidal basis functions with and without the edge singularity condition is also calculated and discussed. The obtained results for the real and imaginary parts of the complex resonant frequencies are analyzed as functions of the superstrate permittivity and thickness. The results are also compared with those obtained for the superstrate-loaded planar microstrip structure [9] to analyze the curvature effect on the resonant frequency, radiation loss, and quality factor of a conformal microstrip structure.

Manuscript received June 22, 1992; revised September 3, 1992. This work was supported by the National Science Council of the Republic of China under Grant NSC81-0404-E110-544.

The authors are with the Department of Electrical Engineering, National Sun Yat-Sen University, Kaohsiung, Taiwan 804, Republic of China.

IEEE Log Number 9207418.

II. Full-Wave Formulation of the Problem

Fig. 1 shows the geometry of a cylindrical-rectangular microstrip patch loaded with a protecting dielectric superstrate. The cylindrical microstrip structure considered here is a concentric circular cylindrical structure consisting of a ground perfect conducting cylinder with radius a (region 0) and coaxial cylindrical substrate (region 1) and superstrate (region 2) layers. The air is in region 3 with free space permittivity ϵ_0 and permeability μ_0. The curved rectangular patch is at the substrate-superstrate interface of $\rho = b$ and has a straight dimension of $2L$ and a curved dimension of $2b\phi_0$, where $2\phi_0$ is the angle subtended by the curved patch. The substrate layer is with a relative permittivity ϵ_1 and thickness $h\,(=b-a)$, while the superstrate layer is of thickness $t\,(=c-b)$ and a relative permittivity ϵ_2. The permeability is everywhere assumed to be μ_0. In this geometry the z components of the electric and magnetic fields in each region can be given by (suppressing $e^{-j\omega t}$ time dependence)

$$E_z(\rho,\phi,z) = \frac{1}{2\pi}\sum_{n=-\infty}^{\infty} e^{jn\phi}\int_{-\infty}^{\infty} dk_z e^{jkz^z} \cdot \begin{cases} [A_n^e H_n^{(1)}(k_{1\rho}\rho) + B_n^e J_n(k_{1\rho}\rho)], & b>\rho>a \quad (1a)\\ [C_n^e H_n^{(1)}(k_{2\rho}\rho) + D_n^e J_n(k_{2\rho}\rho)], & c>\rho>b \quad (1b)\\ G_n^e H_n^{(1)}(k_{3\rho}\rho), & \rho>c \quad (1c)\end{cases}$$

$$H_z(\rho,\phi,z) = \frac{1}{2\pi}\sum_{n=-\infty}^{\infty} e^{jn\phi}\int_{-\infty}^{\infty} dk_z e^{jkz^z} \cdot \begin{cases} [A_n^h H_n^{(1)}(k_{1\rho}\rho) + B_n^h J_n(k_{1\rho}\rho)], & b>\rho>a \quad (2a)\\ [C_n^h H_n^{(1)}(k_{2\rho}\rho) + D_n^h J_n(k_{2\rho}\rho)], & c>\rho>b \quad (2b)\\ G_n^h H_n^{(1)}(k_{3\rho}\rho), & \rho>c \quad (2c)\end{cases}$$

where $k_i^2 - k_{i\rho}^2 = k_z^2, i = 1,2,3$, and there are ten unknown coefficients of $A_n^x, B_n^x, C_n^x, D_n^x$ and $G_n^x, x = e,h$, to be determined. From the expressions of E_z and H_z the components E_ϕ and H_ϕ can also be expressed as

$$E_\phi = \frac{-j\omega\mu_0}{k_{i\rho}^2}\frac{dH_z}{d\rho} - \frac{k_z n}{k_{i\rho}^2\rho}E_z, \quad (3a)$$

$$H_\phi = \frac{j\omega\epsilon}{k_{i\rho}^2}\frac{dE_z}{d\rho} - \frac{k_z n}{k_{i\rho}^2\rho}H_z. \quad (3b)$$

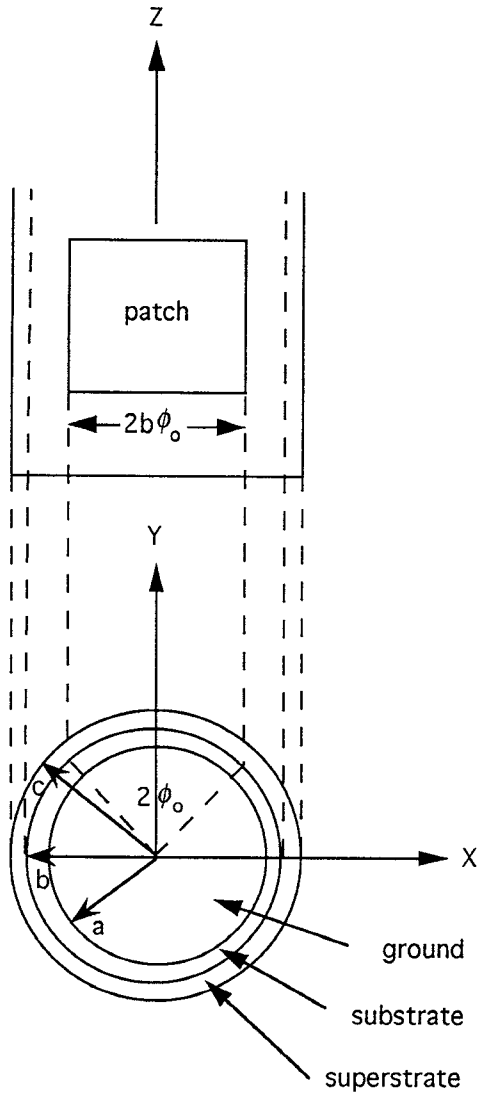

Fig. 1. The geometry of a cylindrical-rectangular microstrip patch with a dielectric superstrate cover.

Imposing the boundary conditions at $\rho = a, b$, and c for the E_z and E_ϕ components of the electric field, we can have the coefficients of A_n^x, B_n^x, C_n^x, and D_n^x for E_z and H_z to be expressed in terms of G_n^x and given in Appendix I. These coefficients for a vanishing superstrate layer (i.e., $c \to b$) can be reduced to the corresponding values shown in [2].

As for applying the discontinuity boundary condition at $\rho = b$ for the tangential components H_z and H_ϕ of the magnetic field on the patch, a matrix relationship between the current density in the spectral domain on the patch and the field amplitudes in region 3 can be obtained and given by

$$\begin{bmatrix} J_{\phi n}(k_z) \\ J_{zn}(k_z) \end{bmatrix} = \begin{bmatrix} X_{11} & X_{12} \\ X_{21} & X_{22} \end{bmatrix} \cdot \begin{bmatrix} G_n^e H_n^{(1)}(k_{3\rho}) \\ G_n^h H_n^{(1)}(k_{3\rho}) \end{bmatrix}. \quad (4)$$

where the coefficients X_{11}, X_{12}, X_{21}, and X_{22} are listed in Appendix II and

$$\begin{bmatrix} J_{\phi n}(k_z) \\ J_{zn}(k_z) \end{bmatrix} = \frac{1}{2\pi} \int_{-\pi}^{\pi} d\phi\, e^{-jn\phi} \int_{-\infty}^{\infty} dz\, e^{-jkz} \begin{bmatrix} J_{\phi n}(\phi, z) \\ J_{zn}(\phi, z) \end{bmatrix}. \quad (5)$$

Furthermore, following the derivation procedure in [2], the tangential components of the electric field, $E_{\phi n}$ and E_{zn} in the spectral domain, on the patch can be found to be related to the current density $J_{\phi n}$ and J_{zn} in (5) and the following equation is obtained:

$$\begin{bmatrix} E_{\phi n}(k_z) \\ E_{zn}(k_z) \end{bmatrix} = \overline{\overline{Q}}_n(k_z) \cdot \begin{bmatrix} J_{\phi n}(k_z) \\ J_{zn}(k_z) \end{bmatrix}, \quad (6)$$

where

$$\overline{\overline{Q}}_n(k_z) = \begin{bmatrix} Q_{\phi\phi} & Q_{\phi z} \\ Q_{z\phi} & Q_{zz} \end{bmatrix} = \begin{bmatrix} S_{11} & S_{12} \\ S_{21} & S_{22} \end{bmatrix} \begin{bmatrix} X_{11} & X_{12} \\ X_{21} & X_{22} \end{bmatrix}^{-1} \quad (7)$$

and

$$\begin{bmatrix} E_{\phi n}(k_z) \\ E_{zn}(k_z) \end{bmatrix} = \frac{1}{2\pi} \int_{-\pi}^{\pi} d\phi\, e^{-jn\phi} \int_{-\infty}^{\infty} dz\, e^{-jkz} \begin{bmatrix} E_{\phi n}(\phi, z) \\ E_{zn}(\phi, z) \end{bmatrix}. \quad (8)$$

The coefficients S_{11}, S_{12}, S_{21}, and S_{22} in (7) are also listed in Appendix II. Next, by imposing the boundary condition on the patch and outside the patch at the substrate-superstrate interface, the following integral equations can be obtained:

$$\begin{bmatrix} E_{\phi n}(\phi, z) \\ E_{zn}(\phi, z) \end{bmatrix} = \frac{1}{2\pi} \sum_{n=-\infty}^{\infty} e^{jn\phi} \int_{-\infty}^{\infty} dk_z e^{jk_z z} \overline{\overline{Q}}_n(k_z) \begin{bmatrix} J_{\phi n}(k_z) \\ J_{zn}(k_z) \end{bmatrix} = \begin{bmatrix} 0 \\ 0 \end{bmatrix}, \quad (9)$$

and, outside the patch,

$$\begin{bmatrix} J_\phi(\phi, z) \\ J_z(\phi, z) \end{bmatrix} = \frac{1}{2\pi} \sum_{n=-\infty}^{\infty} e^{jn\phi} \int_{-\infty}^{\infty} dk_z\, e^{jkz} \begin{bmatrix} J_{\phi n}(k_z) \\ J_{zn}(k_z) \end{bmatrix} = \begin{bmatrix} 0 \\ 0 \end{bmatrix}. \quad (10)$$

To solve for the above integral equations, the Galerkin's moment method [10] is applied. Following the Galerkin's calculation procedure, we first expand the surface current density on the patch in terms of linear combinations of known basis functions, i.e.

$$\vec{J}(\phi, z) = \sum_{n=1}^{N} I_{\phi n} \vec{J}_{\phi n}(\phi, z) + \sum_{m=1}^{M} I_{zm} \vec{J}_{zm}(\phi, z), \quad (11)$$

where $I_{\phi n}$ and I_{zm} are unknown coefficients for the nth expansion mode of the basis functions $J_{\phi n}$ and J_{zm} in the ϕ and z directions, respectively. A convenient choice of the basis functions is the cavity mode functions of

$$\vec{J}_{\phi n}(\phi, z) = \hat{\phi} \sin\left[\frac{p\pi}{2\phi_0}(\phi - \phi_0)\right] \cos\left[\frac{q\pi}{2L}(z + L)\right], \quad (12a)$$

$$\vec{J}_{zm}(\phi, z) = z \sin\left[\frac{r\pi}{2L}(z + L)\right] \cos\left[\frac{s\pi}{2\phi_0}(\phi - \phi_0)\right], \quad (12b)$$

or

$$\vec{J}_{\phi n}(\phi,z)=\hat{\phi}\frac{1}{\sqrt{L^2-z^2}}\sin\left[\frac{p\pi}{2\phi_0}(\phi-\phi_0)\right]\cos\left[\frac{q\pi}{2L}(z+L)\right], \tag{13a}$$

$$\vec{J}_{zm}(\phi,z)=\hat{z}\frac{1}{\sqrt{\phi_0^2-\phi^2}}\sin\left[\frac{r\pi}{2L}(z+L)\right]\cos\left[\frac{s\pi}{2\phi_0}(\phi-\phi_0)\right]. \tag{13b}$$

The sinusoidal basis functions of (13) consider the edge singularity condition for the tangential component of the surface current at the edge of the patch, while the basis functions of (12) do not consider such edge singularity conditions. The combinations of the integers p, q, r, and s depend on the mode numbers n and m. For the first three modes, $n = 1, 2$, and 3, the values of (p, q) are (1, 0), (1, 1) and (1, 2), respectively, and the values of (r, s) are (1, 0), (1, 1) and (1, 2) for $m = 1, 2$ and 3. The numerical convergence for the sinusoidal basis functions with and without considering the edge singularity condition will be calculated and discussed in detail in Section III. Next, by taking the spectral amplitudes of the selected basis functions and substituting into (9), we have

$$\sum_{r=-\infty}^{\infty} e^{jr\phi}\int_{-\infty}^{\infty} dk_z\, e^{jkz^z}\overline{\overline{Q}}_r(k_z)\cdot\begin{bmatrix}\sum_{n=1}^{N} I_{\phi n}F_{\phi n,r}(k_z)\\ \sum_{m=1}^{M} I_{zm}F_{zm,r}(k_z)\end{bmatrix} = \begin{bmatrix}0\\0\end{bmatrix}, \tag{14}$$

where

$$F_{\phi n,r}(k_z)=\frac{1}{2\pi}\int_{-\pi}^{\pi} d\phi\, e^{-jr\phi}\int_{-L}^{L} dz\, e^{-jkz^z}J_{\phi n}(\phi,z), \tag{15}$$

$$F_{zm,r}(k_z)=\frac{1}{2\pi}\int_{-\pi}^{\pi} d\phi\, e^{-jr\phi}\int_{-L}^{L} dz\, e^{-jkz^z}J_{zm}(\phi,z). \tag{16}$$

Using the selected basis functions as testing functions and integrating over the patch area, we can have the following homogeneous matrix equation

$$\begin{bmatrix}(Z_{ln}^{\phi\phi})_{N\times N} & (Z_{ln}^{\phi z})_{N\times M}\\ (Z_{kn}^{z\phi})_{M\times N} & (Z_{km}^{zz})_{M\times M}\end{bmatrix}\cdot\begin{bmatrix}(I_{\phi n})_{N\times 1}\\ (I_{zm})_{M\times 1}\end{bmatrix}=\begin{bmatrix}0\\0\end{bmatrix}, \tag{17}$$

where

$$Z_{ln}^{\phi\phi}=\int_{-\infty}^{\infty}dk_z\sum_{r=-\infty}^{\infty}F_{\phi l,r}(k_z^*)Q_{\phi\phi}F_{\phi n,r}(k_z), \tag{18a}$$

$$Z_{lm}^{\phi z}=\int_{-\infty}^{\infty}dk_z\sum_{r=-\infty}^{\infty}F_{\phi l,r}(k_z^*)Q_{\phi z}F_{zm,r}(k_z), \tag{18b}$$

$$Z_{kn}^{z\phi}=\int_{-\infty}^{\infty}dk_z\sum_{r=-\infty}^{\infty}F_{zk,r}(k_z^*)Q_{z\phi}F_{\phi n,r}(k_z), \tag{18c}$$

$$Z_{km}^{zz}=\int_{-\infty}^{\infty}dk_z\sum_{r=-\infty}^{\infty}F_{zk,r}(k_z^*)Q_{zz}F_{zm,r}(k_z), \quad k,m=1,2,\cdots,M, \quad l,n=1,2,\cdots,N. \tag{18d}$$

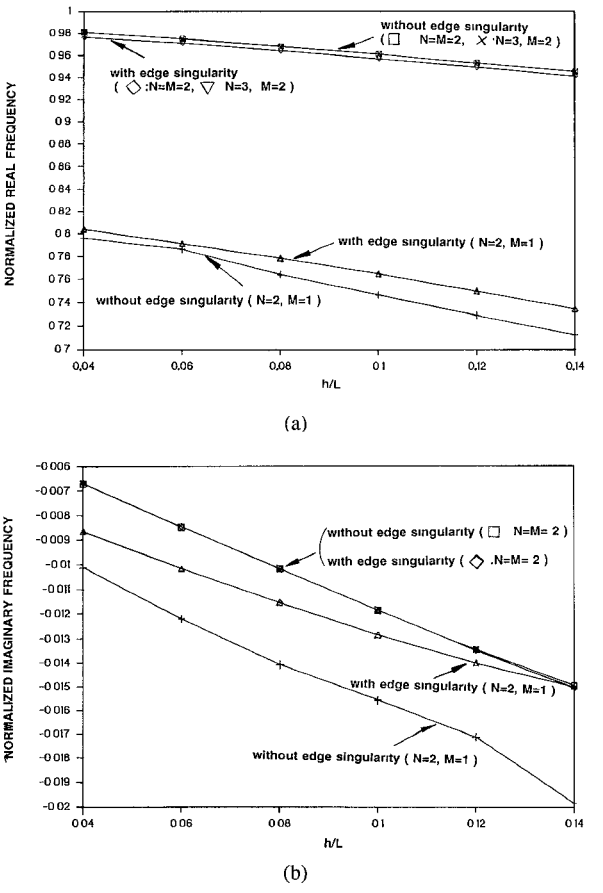

Fig. 2. Normalized frequency shifts with different numbers of the sinusoidal basis functions with and without the edge singularity condition versus substrate thickness; $a = 20$ cm, $L = 4$ cm, $b\phi_0 = 8.4$ cm, $\epsilon_1 = 2.3$. (a) Real resonant frequency. (b) Imaginary resonant frequency.

There exist nontrivial solutions for $I_{\phi n}$ and I_{zm} in (17) if the determinant of (17) vanishes, i.e

$$\det\begin{bmatrix}(Z_{ln}^{\phi\phi})_{N\times N} & (Z_{lm}^{\phi z})_{N\times M}\\ (Z_{kn}^{z\phi})_{M\times M} & (Z_{km}^{zz})_{M\times M}\end{bmatrix}=0. \tag{19}$$

The solutions to (19) are then found to be satisfied by complex frequencies. For a particular mode, the complex frequency is $f = f' + jf$ that gives the resonant frequency f' and the quality factor $f'/2f''$ for the superstrate-loaded cylindrical-rectangular microstrip structure.

III. Numerical Results and Discussion

In this section, typical numerical results of the superstrate-loaded cylindrical-rectangular microstrip patch at the HE_{01} mode are presented and analyzed. The hybrid mode HE_{01} tends to the TE_{01} mode for the case of vanishing thin substrates, which is shown to be an efficient radiating mode [2]. The numerical convergence and the computer computation time for the calculation with the sinusoidal basis functions of (12) and (13), respectively, are first studied. Fig. 2 shows the real and imaginary parts of the complex resonant frequencies obtained for different numbers of the sinusoidal basis functions with and without the edge singularity condition versus the substrate thickness. The substrate is with a relative permittivity of 2.3 and the radius of the ground conducting cylinder is

chosen to be 20 cm. The cylindrical-rectangular microstrip patch considered in the calculation is with a straight dimension of $2L = 8$ cm and a curved dimension of $2b\phi_0 = 16.8$ cm. The frequencies are all normalized with respect to the cavity-mode resonant frequency [11]. It is observed that both the real and imaginary resonant frequencies can only reach convergent solutions for both the basis functions of (12) and (13) with $N \geq 2$ and $M \geq 2$. It is also found that the computer computation time for reaching the convergent solution of one resonant frequency ($N = M = 2$) on a HP720 workstation is about the same and is estimated to be about 700 seconds. The real parts of the convergent solutions using basis functions with edge singularity are also found to differ from those without edge singularity with about 0.5%, while the imaginary parts of the convergent solutions for both types of the basis function are almost exactly the same. The convergent results are also in good agreement with those presented in [2]. It is also noted that, for $N = 2, M = 1$, the obtained results of the basis function with edge singularity are seen to be much closer to the convergent results than those obtained by using the basis functions without edge singularity, especially for the imaginary parts of the results and the higher thickness of the substrate. This may imply that the sinusoidal basis functions considering the edge singularity can describe the unknown surface current on the cylindrical-rectangular patch more accurately.

Fig. 3 shows the normalized real and imaginary parts of the complex resonant frequencies versus the superstrate thickness for $\epsilon_2 = 2.3, 4.0$, and 5.6 with $a = 20, \infty$ cm. The substrate thickness h is 0.4 cm and the relative permittivity ϵ_1 is 2.3. The results for the planar microstrip case ($a = \infty$ cm) are obtained in [9], which is based on a rigorous Green's function formulation and moment method calculation. The basis functions of (13) with $N = M = 2$ are used to obtain the results. It can be seen that the real (resonant) frequency decreases as the superstrate permittivity increases and the curved microstrip case is with a higher resonant frequency than that for the planar microstrip case. From the imaginary results in Fig. 3(b), it is seen that the radiation loss of the cylindrical-rectangular microstrip structure at HE_{01} mode is higher than that for the planar microstrip case and can be further increased when a higher superstrate permittivity is used. The variations of the quality factor with the superstrate thickness for the case in Fig. 3 are shown in Fig. 4. The quality factor is seen to decrease when the superstrate permittivity is higher, and the curved microstrip case is with a lower quality factor than that for the planar microstrip case.

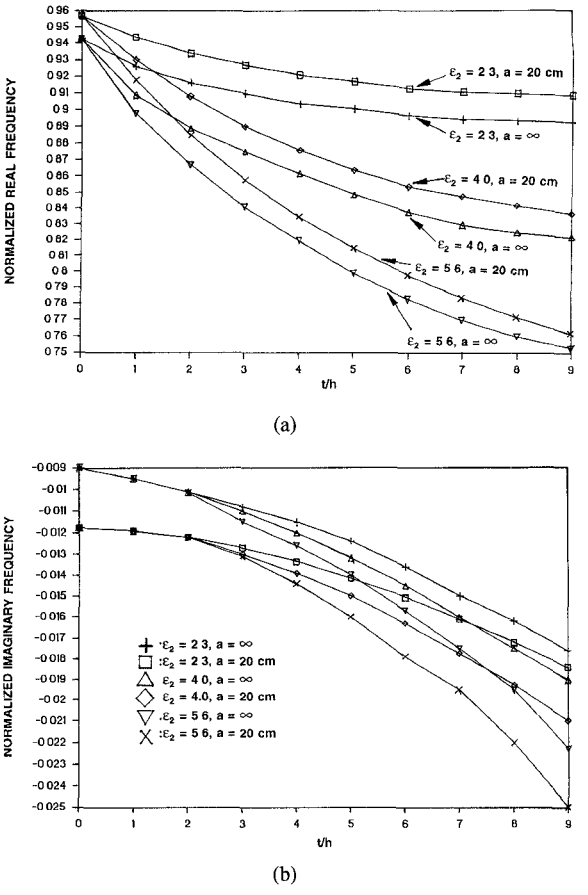

Fig. 3. Normalized frequency shifts versus the superstrate thickness for $\epsilon_2 = 2.3, 4.0$, and 5.6; $a = 20, \infty$ cm. (a) Real resonant frequency. (b) Imaginary resonant frequency. The results for the planar microstrip case ($a = \infty$ cm) are obtained in [9].

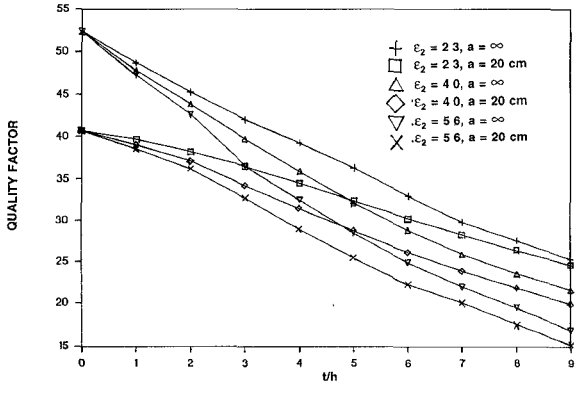

Fig. 4. Variations of the quality factor with the superstrate thickness for the case in Fig. 3.

IV. Conclusions

A full-wave approach and the Galerkin's moment method are employed to solve the complex resonant frequency for a superstrate-loaded cylindrical-rectangular microstrip structure. The sinusoidal basis functions with the edge singularity are found to be more appropriate for expanding the unknown surface current on the cylindrical-rectangular patch. Numerical results also indicate that both the resonant frequency and the radiation loss of the curved microstrip structure are higher than those of the planar case. On the contrary, the quality factor of the curved structure is lower than that of the planar case. On the other hand, as the superstrate permittivity increases, both the resonant frequency and the quality factor decrease and the radiation loss, however, increases.

Appendix I

The coefficients A_n^x, B_n^x, C_n^x, and $D_n^x, x = e, h$, for E_z and H_z in regions 1 and 2 can be expressed in terms of G_n^x in

region 3 and given by

$$A_n^e = J_n(k_{1\rho}a)[C_n^e H_n^{(1)}(k_{2\rho}b) + D_n^e J_n(k_{2\rho}b)]/[J_n(k_1\rho a)H_n^{(1)}(k_{1\rho}b) - J_n(k_{1\rho}b)H_n^{(1)}(k_{1\rho}a)],$$

$$A_n^h = \frac{J_n'(k_{1\rho}a)[C_n^h H_n^{(1)'}(k_{2\rho}b) + D_n^h J_n'(k_{2\rho}b)]}{J_n'(k_{1\rho}a)H_n^{(1)'}(k_{1\rho}b) - J_n'(k_{1\rho}b)H_n^{(1)'}(k_{1\rho}a)}\frac{k_{1\rho}}{k_{2\rho}} - \frac{j\omega\epsilon_2 k_z n}{k_{1\rho}k_{2\rho}^2 b}\left(\frac{\epsilon_1}{\epsilon_2} - 1\right)[C_n^e H_n^{(1)}(k_{2\rho}b) + D_n^e J_n(k_{2\rho}b)],$$

$$B_n^e = -\frac{H_n^{(1)}(k_{1\rho}a)}{J_n(k_{1\rho}a)}A_n^e,$$

$$B_n^h = \frac{H_n^{(1)'}(k_{1\rho}a)}{J_n'(k_{1\rho}a)}A_n^h,$$

$$C_n^e = \alpha_1 G_n^e + \alpha_2 G_n^h,$$

$$C_n^h = \alpha_3 G_n^e + \alpha_4 G_n^h,$$

$$D_n^e = \frac{-\alpha_3 H_n(k_{2\rho}c)}{J_n(k_{2\rho}c)}G_n^e + \frac{1 - \alpha_4 H_n^{(1)}(k_{2\rho}c)}{J_n(k_{2\rho}c)}G_n^h,$$

$$D_n^h = \frac{1 - \alpha_3 H_n(k_{2\rho}c)}{J_n(k_{2\rho}c)}G_n^e - \frac{\alpha_4 H_n^{(1)}(k_{2\rho}c)}{J_n(k_{2\rho}c)}G_n^h,$$

where

$$\alpha_1 = \alpha_0\left[\frac{\epsilon_3 k_{2\rho}H_n^{(1)'}(k_{3\rho}c)}{\epsilon_2 k_{3\rho}H_n^{(1)}(k_{3\rho}c)} - \frac{J_n'(k_{2\rho}c)}{J_n(k_{2\rho}c)}\right],$$

$$\alpha_2 = \alpha_0\frac{j\omega\mu_0 k_z n}{k_{3\rho}^2 k_{2\rho}c}\left(\frac{\epsilon_3}{\epsilon_2} - 1\right),$$

$$\alpha_3 = \left[\frac{k_{2\rho}H_n^{(1)'}(k_{3\rho}c)}{k_{3\rho}H_n^{(1)}(k_{3\rho}c)} - \frac{J_n'(k_{2\rho}c)}{J_n(k_{2\rho}c)}\right]$$

$$\alpha_4 = \frac{j\omega\epsilon_3 k_z n}{k_{3\rho}^2 k_{2\rho}b}\left(1 - \frac{\epsilon_2}{\epsilon_3}\right),$$

$$\alpha_0 = \frac{J_n(k_{2\rho}c)}{H_n^{(1)'}(k_{2\rho}c)J_n(k_{2\rho}c) - J_n'(k_{2\rho}c)H_n^{(1)}(k_{2\rho}c)}.$$

APPENDIX II

The coefficients $X_{11}, X_{12}, X_{21}, X_{22}, S_{11}, S_{12}, S_{21}, S_{22}$ are expressed as

$$X_{11} = \beta_1 X_0/\beta_0 - y_2\beta_4,$$

$$X_{12} = \beta_2 X_0/\beta_0 - [y_3\beta_4 + J_n(k_{2\rho}b)/J_n(k_{2\rho}c)],$$

$$X_{21} = \frac{jk_0}{120\pi}\left\{\frac{\epsilon_{23}}{k_{2\rho}}\left[y_0\beta_3 + \frac{J_n'(k_{2\rho}b)}{J_n(k_{2\rho}c)}\right] - \frac{\epsilon_{13}}{k_{1\rho}}\beta_0 X_1\left[y_0\beta_4 + \frac{J_n(k_{2\rho}b)}{J_n(k_{2\rho}c)}\right]\right\} + \frac{nk_z}{b}\left\{\frac{\beta_1}{k_{1\rho}^2\beta_0}X_0 - \frac{y_2\beta_4}{k_{2\rho}^2}\right\}$$

$$X_{22} = \frac{jk_0}{120\pi}\left[\frac{\epsilon_{23}}{k_{2\rho}}y_1\beta_3 + \frac{\epsilon_{13}}{k_{1\rho}}y_1\beta_4\beta_0 X_1\right] + \frac{nk_z}{b}\left[\frac{\beta_5}{k_{1\rho}^2\beta_0}X_0 - \frac{1}{k_{2\rho}^2}\left(y_3\beta_4 + \frac{J_n(k_{2\rho}b)}{J_n(k_{2\rho}c)}\right)\right],$$

$$S_{11} = -\frac{nk_z}{k_{1\rho}^2 b}\left[y_0\beta_4 + \frac{J_n(k_{2\rho}b)}{J_n(k_{2\rho}c)}\right] - \frac{j120\beta_1 k_0}{k_{1\rho}},$$

$$S_{12} = -\frac{nk_z}{k_{1\rho}^2 b}y_1\beta_4 - \frac{j120\pi\beta_5 k_0}{k_{1\rho}},$$

$$S_{21} = y_0\beta_4 + \frac{J_n(k_{2\rho}b)}{J_n(k_{2\rho}c)},$$

$$S_{22} = y_1\beta_4,$$

where

$$X_0 = \frac{J_n'(k_{1\rho}b)}{J_n(k_{1\rho}b)}\frac{H_n^{(1)}(k_{1\rho}b)J_n'(k_{1\rho}a) - H_n^{(1)'}(k_{1\rho}a)J_n(k_{1\rho}b)}{H_n^{(1)'}(k_{1\rho}b)J_n(k_{1\rho}a) - H_n^{(1)'}(k_{1\rho}b)J_n'(k_{1\rho}b)},$$

$$X_1 = \frac{J_n(k_{1\rho}b)}{J_n'(k_{1\rho}b)}\frac{H_n^{(1)'}(k_{1\rho}b)J_n(k_{1\rho}a) - H_n^{(1)'}(k_{1\rho}a)J_n'(k_{1\rho}b)}{H_n^{(1)}(k_{1\rho}b)J_n(k_{1\rho}a) - H_n^{(1)'}(k_{1\rho}a)J_n(k_{1\rho}b)},$$

$$\beta_0 = J_n'(k_{1\rho}b)/J_n(k_{1\rho}b),$$

$$\beta_1 = \frac{nk_z}{j120\pi k_0 k_{1\rho}b}\left(\frac{k_{1\rho}^2}{k_{2\rho}^2} - 1\right)\left(y_0\beta_4 + \frac{J_n(k_{2\rho}b)}{J_n(k_{2\rho}c)}\right) + \frac{k_{1\rho}}{k_{2\rho}}y_2\beta_4,$$

$$\beta_2 = J_n'(k_{2\rho}c)/J_n(k_{2\rho}c),$$

$$\beta_3 = H_n^{(1)'}(k_{2\rho}b) - J_n'(k_{2\rho}b)H_n^{(1)}(k_{2\rho}c)/J_n(k_{2\rho}c),$$

$$\beta_4 = H_n^{(1)}(k_{2\rho}b) - J_n(k_{2\rho}b)H_n^{(1)}(k_{2\rho}c)/J_n(k_{2\rho}c),$$

$$\beta_5 = \frac{nk_z}{j120\pi k_0 k_{1\rho} b}\left(\frac{k_{1\rho}^2}{k_{2\rho}^2} - 1\right) y_1\beta_4 + \frac{k_{1\rho}}{k_{2\rho}}\left[y_3\beta_3 + \frac{J_n'(k_{2\rho}b)}{J_n(k_{2\rho}c)}\right],$$

$$\beta_6 = H_n^{(1)'}(k_{2\rho}c)/H_n^{(1)}(k_{2\rho}c),$$

$$\beta_7 = H_n^{(1)'}(k_{3\rho}c)/H_n^{(1)}(k_{3\rho}c),$$

$$\epsilon_{13} = \epsilon_1/\epsilon_3, \epsilon_{23} = \epsilon_2/\epsilon_3,$$

$$y_0 = \frac{1}{\beta_2 - \beta_6}\frac{1}{H_n^{(1)}(k_{2\rho}c)}\left(\beta_2 - \frac{k_{2\rho}}{k_{3\rho}\epsilon_{23}}\right),$$

$$y_1 = \frac{1}{\beta_2 - \beta_6}\frac{1}{H_n^{(1)}(k_{2\rho}c)}(k_{2\rho}^2/k_{3\rho}^2 - 1)\frac{120\pi nk_z}{jk_0\epsilon_{23}k_{2\rho}c},$$

$$y_2 = \frac{1}{\beta_2 - \beta_6}\frac{1}{H_n^{(1)}(k_{2\rho}c)}(1 - k_{2\rho}^2/k_{3\rho}^2)\frac{nk_z}{jk_0 120\pi k_{2\rho}c},$$

$$y_3 = \frac{1}{\beta_2 - \beta_6}\frac{1}{H_n^{(1)}(k_{2\rho}c)}(\beta_2 - \beta_7 k_{2\rho}/k_{3\rho}).$$

REFERENCES

[1] K. M. Luk, K. F. Lee, and J. S. Dahele, "Analysis of the cylindrical-rectangular patch antenna," *IEEE Trans. Antennas Propagat.*, vol. 37, pp. 143–147, Feb. 1989.

[2] S. M. Ali, T. M. Habashy, J. F. Kiang, and J. A. Kong, "Resonance in cylindrical-rectangular and wraparound microstrip structures," *IEEE Trans. Microwave Theory Tech.*, vol. 37, pp. 1773–1783, Nov. 1989.

[3] T. M. Habashy, S. M. Ali, and J. A. Kong, "Input impedance and radiation pattern of cylindrical-rectangular and wraparound microstrip antennas," *IEEE Trans. Antennas Propagat.*, vol. 38, pp. 722–731, May 1990.

[4] F. C. Silva, S. B. A. Fonseca, A. J. M. Soares, and A. J. Giarola, "Analysis of microstrip antennas on circular-cylindrical substrates with a dielectric overlay," *IEEE Trans. Antennas Propagat.*, vol. 39, pp. 1398–1403, 1991.

[5] C. M. Krowne, "Cylindrical-rectangular microstrip antenna," *IEEE Trans. Antennas Propagat.*, vol. AP-31, pp. 194–199, Jan. 1983.

[6] A. Bhattacharyya and T. Tralman, "Effects of dielectric superstrate on patch antennas," *Electron. Lett.*, vol. 24, pp. 356–358, 1988.

[7] K. M. Luk, W. Y. Tam and C. L. Yip, "Analysis of circular microstrip antennas with superstrate," *Proc. Inst. Elec. Eng.*, pt. H, vol. 136, pp. 261–262, 1989.

[8] K. L. Wong, W. S. Chen, and W. L. Huang, "The absorption and coupling of an electromagnetic wave incident on a microstrip circuit with superstrate," *IEEE Trans. Electromagn. Compat.*, vol. 34, pp. 17–22, Feb. 1992.

[9] J. S. Row and K. L. Wong, "Resonance in a superstrate-loaded rectangular microstrip structure," *IEEE Trans. Microwave Theory Tech.*, to appear in Aug 1993 issue; also in Tech. Report EMA-92-06-2, EM Wave and Antenna Lab., National Sun Yat-Sen University, June 1992.

[10] R. F. Harrington, *Field Computation by Moment Methods.* New York: Macmillan, 1968.

[11] Y. T. Lo, D. Soloman, and W. F. Richards, "Theory and experiment on microstrip antennas," *IEEE Trans. Antennas Propagat.*, vol. AP-27, pp. 137–145, 1979.

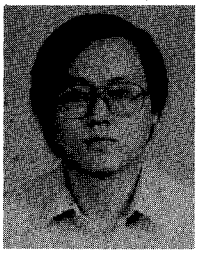

Kin-Lu Wong (M'91) was born in Tainan, Taiwan, in 1959. He received the B.S. degree in electrical engineering from National Taiwan University, Taipei, Taiwan, in 1981, and the M.S. and Ph.D. degrees in electrical engineering from Texas Tech University, Lubbock, TX, in 1984 and 1986, respectively.

From 1986 to 1987 he was a visiting Scientist with Max-Planck-Institut fuer Plasmaphysik in Munich, Germany. In 1987 he was with the Department of Electrical Engineering at National Sun Yat-Sen University, Kaohsiung, Taiwan, where he became a Professor in 1991. His research interests include electromagnetic theory, antenna design, and plasma science.

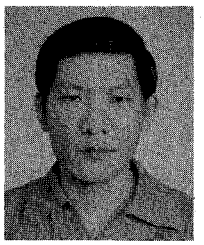

Yuan-Tung Cheng was born in Hong Kong, in 1951. He received the B.S. degree from Chinese Military Academy, Taiwan, Republic of China, in 1973, and the M.S. degree in applied physics from Chung Cheng Institute of Technology, Ta-Hsi, Taiwan, in 1985.

Since then, he has been with the Department of Physics and Chemistry, Chinese Military Academy, Fung-Shan, Taiwan, as a faculty member and he is now pursuing the Ph.D. degree in the Department of Electrical Engineering at the National Sun Yat-Sen University, Kaohsiung, Taiwan. His current research interests are in antenna theory and design, and EM wave propagation.

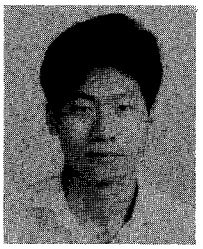

Jeen-Sheen Row was born in Miaoli, Taiwan, Republic of China, in 1967. He received the B.S. degree in electrical engineering from Tamkang University, Taipei, Taiwan, in 1989.

Since 1990 he has been working toward the Ph.D. degree in the Department of Electrical Engineering at the National Sun Yat-Sen University, Kaohsiung. His current research interests are in antenna theory and design, and EM wave propagation.